

## Supporting information

### **Porous rGO/ZnSe/CoSe<sub>2</sub> dispersed in PEDOT:PSS as Efficient Counter Electrode for Dye-Sensitized Solar Cells**

Tapa Arnauld Robert<sup>a</sup>, Wanchun Xiang<sup>\*a, b</sup>, Abdelaal. S. A. Ahmed<sup>a, c</sup>, Senwei Wu<sup>a</sup>, Bin Li<sup>a</sup>, Qiufen Liu<sup>a</sup>, Chawut Machar Jacob Chuti<sup>a, d</sup>, Xiujian Zhao<sup>\*a</sup>

<sup>a</sup> State Key Laboratory of Silicate Materials for Architecture, Wuhan University of Technology, Luoshi Road, Wuhan 430070, P. R. China.

Email : xiangwanchun@whut.edu.cn (W. Xiang), opluse@whut.edu.cn (X. Zhao).

<sup>b</sup> Key Laboratory for Applied Surface and Colloid Chemistry, Ministry of Education; Shaanxi Key Laboratory for Advanced Energy Devices; Shaanxi Engineering Lab for Advanced Energy Technology; School of Materials Science & Engineering, Shaanxi Normal University, Xi'an 710119, P. R. China.

<sup>c</sup> Chemistry Department, Faculty of Science, Al-Azhar University, Assiut, 71524, Egypt.

<sup>d</sup> Chemistry Department, College of Education, University of Bahr el Ghazal, Wau 10739 West Bahr al Ghazal, Republic of South Sudan.

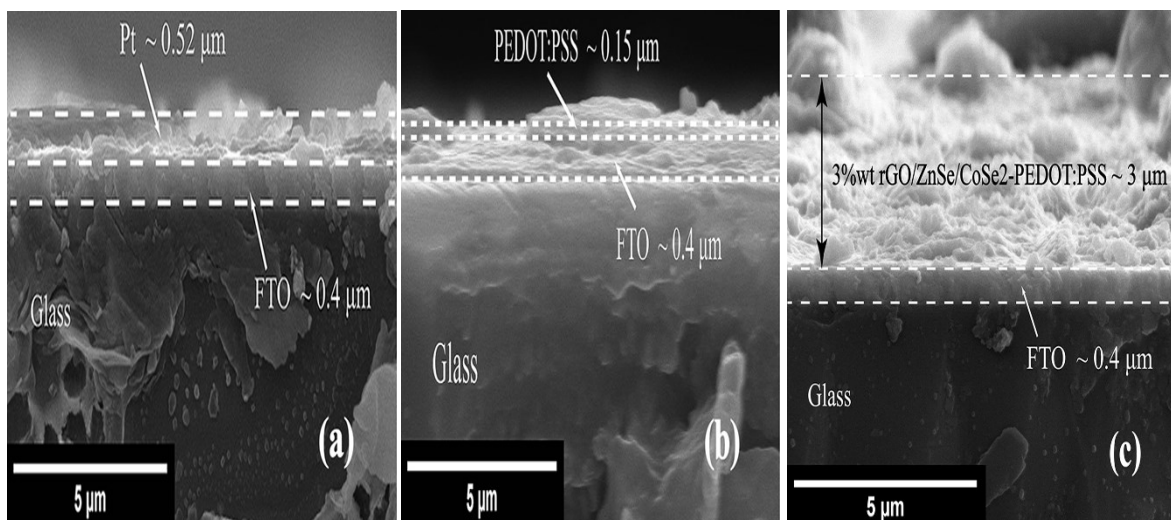


**Fig. S 1** FESEM Cross sectional images of: (a) Pt; (b) PEDOT:PSS; and (c) 3% wt rGO/ZnSe/CoSe<sub>2</sub>-PEDOT:PSS composite.

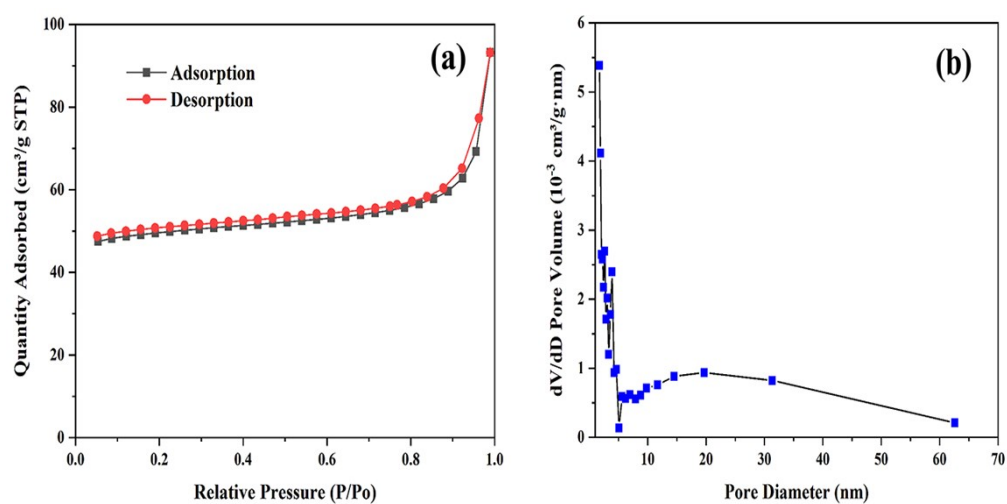


**Fig. S 2** (a) N<sub>2</sub> adsorption-desorption isotherms, and (b) pore-size distributions of rGO/ZnSe/CoSe<sub>2</sub> composite.

**Table S 1** BET parameters for rGO/ZnSe/CoSe<sub>2</sub> composite.

BET	BJH Desorption cumulative surface area of pores	BJH Desorption cumulative volume of pores	BJH Desorption average pore diameter (4V/A)
169.30 m <sup>2</sup> . g <sup>-1</sup>	20.10 m <sup>2</sup> . g <sup>-1</sup>	0.07 cm <sup>3</sup> . g <sup>-1</sup>	14.70 nm

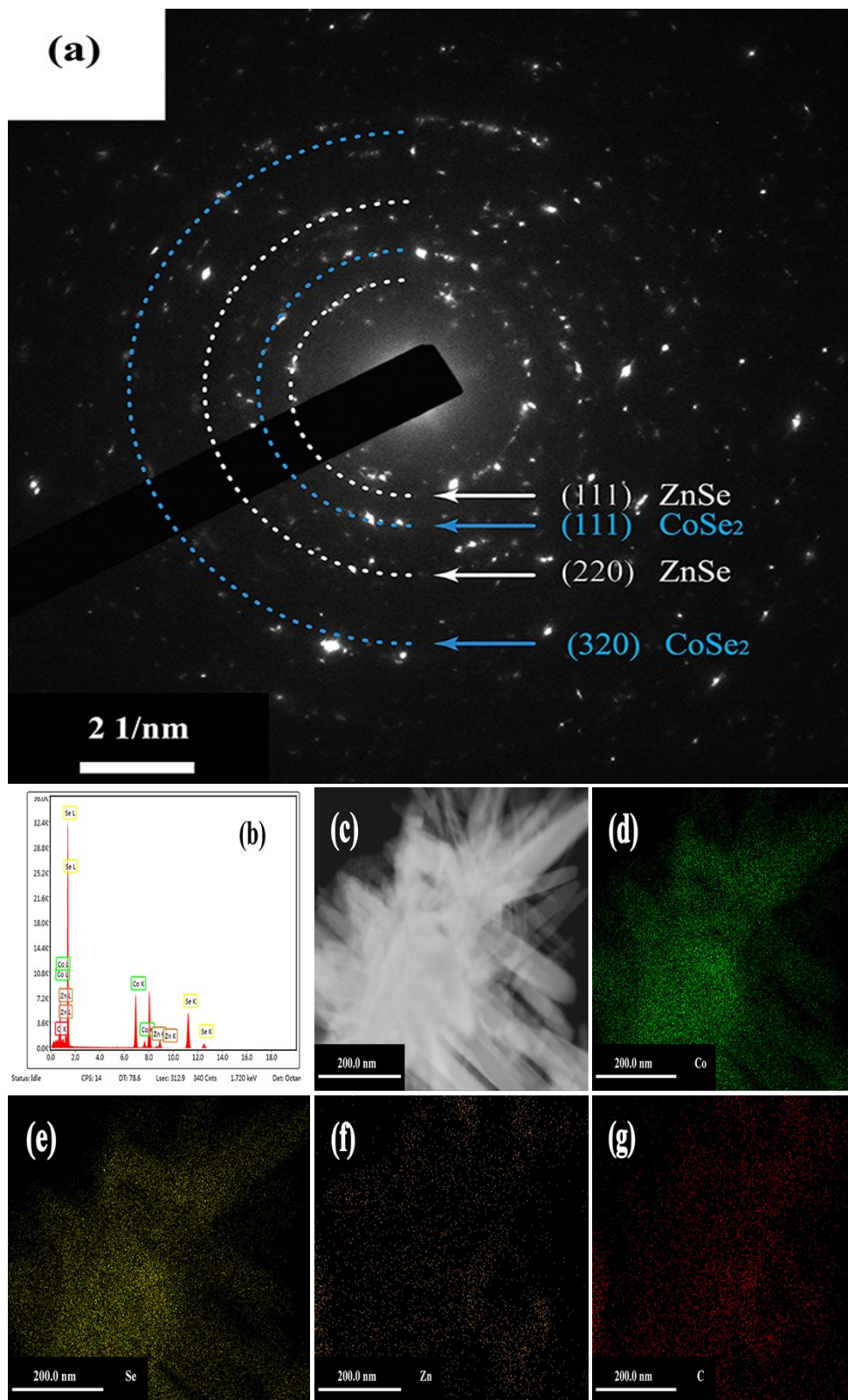


**Fig. S 3** (a) SAED pattern; and (b, c, d, e, f, g) corresponding EDS mapping of porous rGO/ZnSe/CoSe<sub>2</sub>.

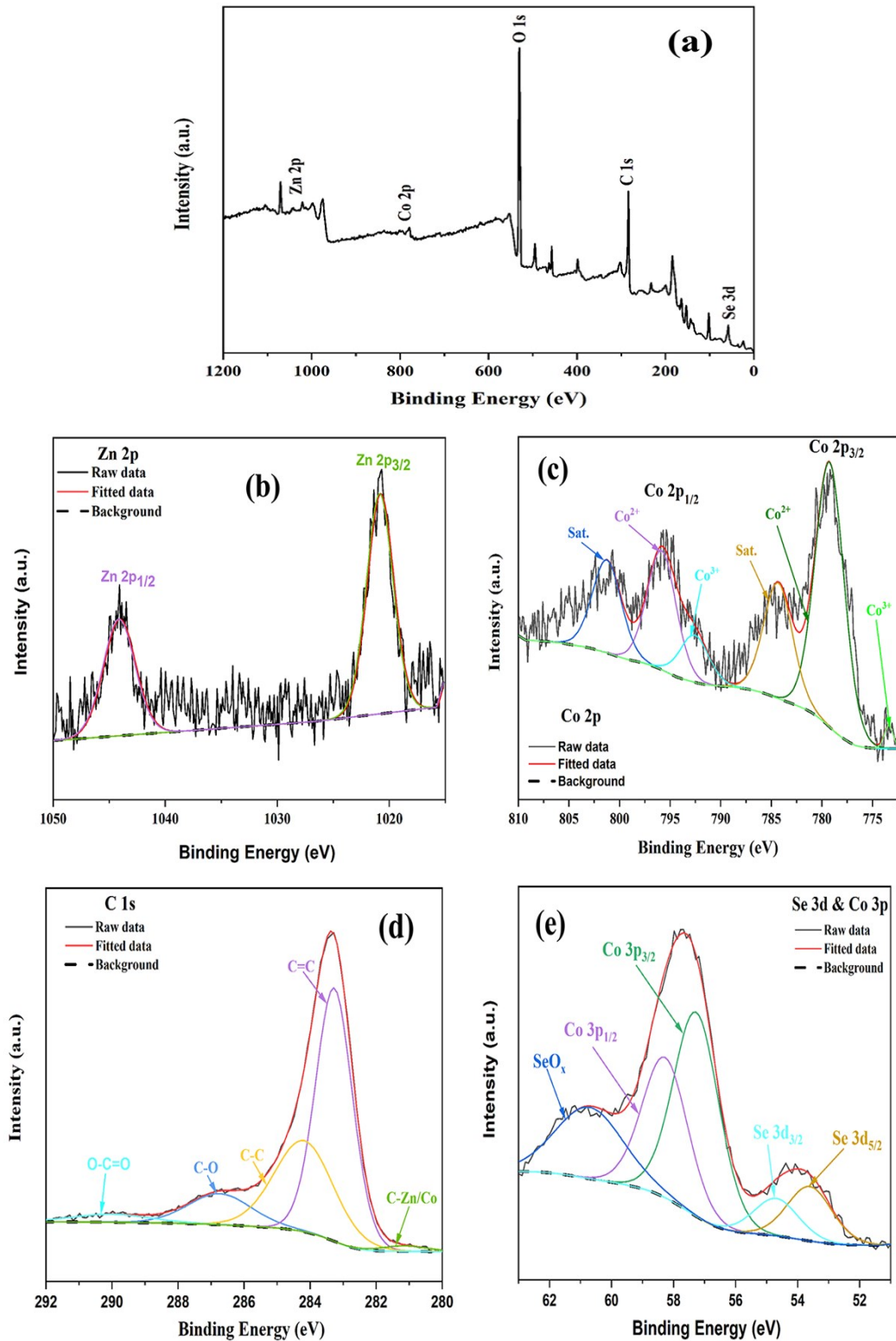


**Fig. S 4** XPS spectra of porous rGO/ZnSe/CoSe<sub>2</sub>: (a) Survey XPS spectra; (b) Zn 2p XPS spectra; (c) Co 2p XPS spectra; (d) C 1s XPS spectra and (e) Se 3d and Co 3p XPS spectra.

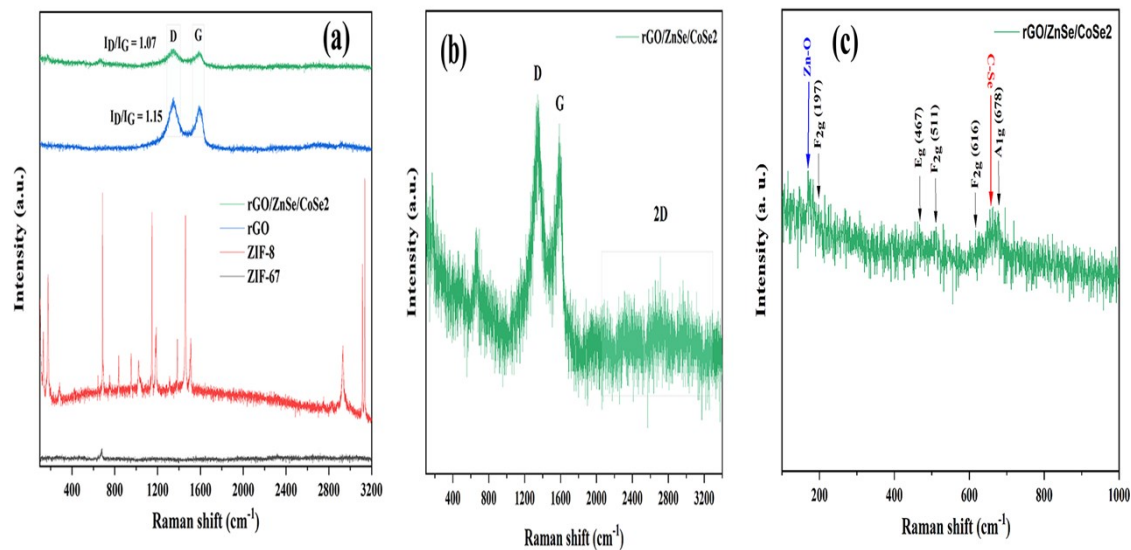


Fig. S 5 Raman spectra of ZIF-8, ZIF-67, rGO, and rGO/ZnSe/CoSe<sub>2</sub>.

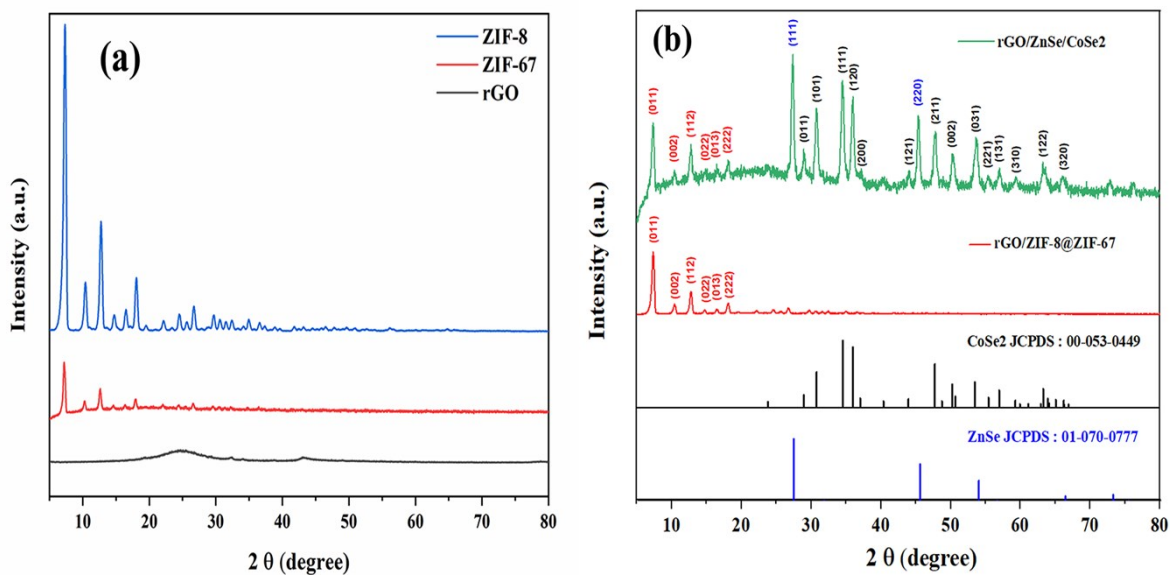
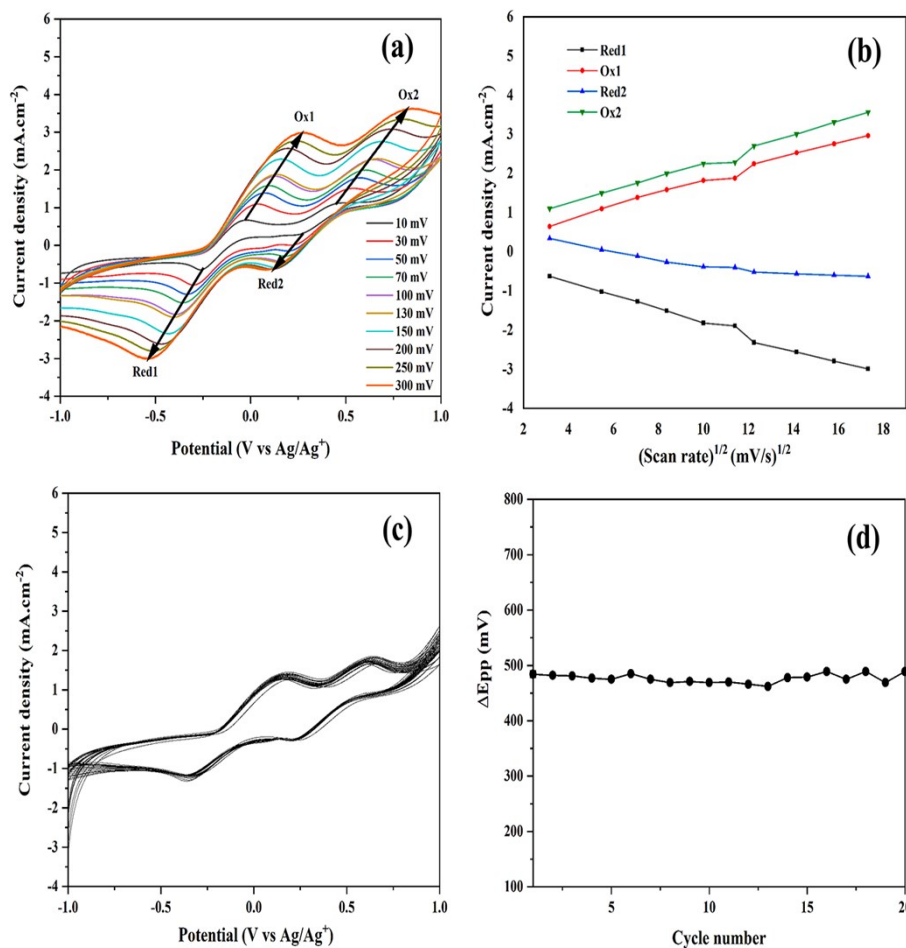
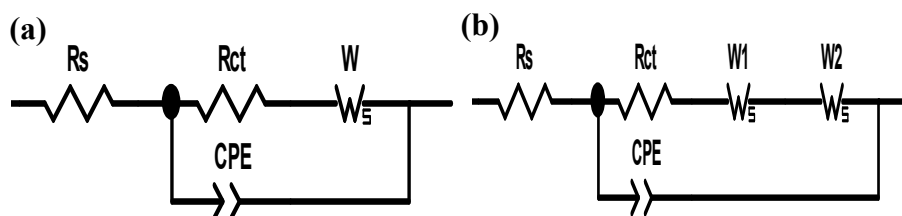


Fig. S 6 XRD patterns of : (a) ZIF-8, ZIF-67 and rGO; (b) rGO/ZIF-8@ZIF-67 and rGO/ZnSe/CoSe<sub>2</sub>.



**Fig. S 7** (a) CV curves of 3% wt rGO/ZnSe/CoSe<sub>2</sub>-PEDOT:PSS CE at different scan rates; (b) Corresponding relationship between peak current densities and the square root of scan rates of 3% wt rGO/ZnSe/CoSe<sub>2</sub>-PEDOT:PSS CE; (c) 20 times consecutive CV curves of 3% wt rGO/ZnSe/CoSe<sub>2</sub>-PEDOT:PSS CE at the 50 mV.s<sup>-1</sup> scan rate in iodine based electrolyte; (d) Corresponding  $\Delta E_{pp}$  values for the 20 times consecutive CV curves of 3% wt rGO/ZnSe/CoSe<sub>2</sub>-PEDOT:PSS CE.



**Fig. S 8** Equivalent circuit models for : (a) Pt and rGO/ZnSe/CoSe<sub>2</sub> symmetric cells; (b) PEDOT:PSS and rGO/ZnSe/CoSe<sub>2</sub>-PEDOT:PSS PSS composites based symmetric cells.